Glow Discharge Source Interfacing to Mass Analyzers: Theoretical and Practical Considerations

ARTICLE *in* ANALYTICAL CHEMISTRY · AUGUST 1999

Impact Factor: 5.64 · DOI: 10.1021/ac9810922 · Source: PubMed

6 AUTHORS, INCLUDING:

Wei Hang
Shanghai University of Finance and Economics
102 PUBLICATIONS **1,318** CITATIONS
SEE PROFILE

Xiaomei Yan
Xiamen University
59 PUBLICATIONS **933** CITATIONS
SEE PROFILE

David Matthew Wayne
Los Alamos National Laboratory
45 PUBLICATIONS **1,122** CITATIONS
SEE PROFILE

José A. Olivares
Los Alamos National Laboratory
35 PUBLICATIONS **1,167** CITATIONS
SEE PROFILE

Anal. Chem. **1999,** *71,* 3231−3237

Glow Discharge Source Interfacing to Mass Analyzers: Theoretical and Practical Considerations

Wei Hang,[†] Xiaomei Yan,[‡] David M. Wayne,*[,†] Jose A. Olivares,[§] W. W. Harrison,[||] and Vahid Majidi[§]

Nuclear Materials and Technology Division, NMT-1, Los Alamos National Laboratory, MS G740, Los Alamos, New Mexico 87545, Life Sciences Division, LS-5, Los Alamos National Laboratory, MS M888, Los Alamos, New Mexico 87545, Chemical Science and Technology Division, CST-9, Los Alamos National Laboratory, MS K484, Los Alamos, New Mexico 87545, and Department of Chemistry, University of Florida, Gainesville, Florida 32611

The fundamental requirements for the optimum mechanical interface between a glow discharge ion source and a mass spectrometer are described in this paper. Specifically, the properties of a typical glow discharge ion source are compared and contrasted to those of a typical inductively coupled plasma ion source. The critical parameters and theoretical considerations of glow discharge and inductively coupled plasma ion source interfaces are reviewed, and the results of experiments using both quadrupole and time-of-flight mass spectrometers with a glow discharge source are presented. The experimental results clarify several important problems in the glow discharge ion sampling process. Our findings indicate that a shock wave structure does not occur in the supersonic expansion of the glow discharge ion source. Ions of different masses have similar initial kinetic energies in the glow discharge; thus, the angle of the skimmer cone is not a critical parameter for efficient ion beam extraction. Another consquence is that space charge effects in glow discharge ion sources repel heavy ions farther off axis than light ions. Thus, there are distinct and fundamental differences between glow discharge and inductively coupled plasma ion sources which are relevant to both ion sampling and ion extraction processes.

The utilization of glow discharges as ion sources for mass spectrometry can be traced back to the 1920s when Aston and his colleagues coupled a glow discharge (GD) source to a mass spectrograph to study the "positive rays" of a low-pressure electrical discharge.[1] Spark source mass spectrometers (SSMS) later emerged as the preferred mass spectrometric method for the direct elemental analysis for solid samples and remained popular until the late 1970s. The renaissance of GD ion sources began in the early 1970s, pioneered by Coburn who used GD sources to explore the physical aspects of plasmas[2] and by Harrison who applied the GD source as an analytical tool.[3] Commercial GD-based mass spectrometers were introduced by several manufacturers in the 1980s, following the commercial appearance of inductively coupled plasma mass spectrometers (ICPMS).[4] Although most commercial GDMS instruments are coupled with double-focusing magnetic sector units, the most recent developments in GDMS have been performed using quadrupole and time-of-flight (TOF) systems.

The GD source permits direct sampling from the solid state, whereas the ICP source requires that samples either be dissolved and nebulized or introduced as a very fine aerosol generated by an intermediate solid sampling technique (e.g., laser ablation, electrothermal vaporization, etc.). In either case, the sample is atomized and ionized in a high-temperature plasma at near-atmospheric pressure. Prior to the development of commercial ICP-based instrumentation, a great deal of theoretical and experimental work was directed toward the development of an efficient atmospheric sampling interface to the analyzer which, in mass spectrometry, must be kept under high vacuum. Analytical GDMS was developed, with minimal research for an appropriate interface, in the wake of commercial ICPMS products. In the rush to establish a foothold for GDMS in the commercial market, manufacturers simply retrofit the GD source to instruments originally optimized for use with electron impact (i.e., for organic analysis), ICP, or thermal ionization (TIMS) sources. The fact that such instruments were viable analytical tools is a testament to the stability, utility, and versatility of the GD source, regardless of the interface configuration. This, however, has led to the unfortunate assumption that the sampling process for the GD source is similar to that of the ICP when, in fact, it is fundamentally different.

The glow discharge is essentially an atom generator that produces a steady-state atomic density via continuous sputtering of the sample by discharge gas (usually Ar) ions.[5] Approximately 90% of the atoms sputtered from the sample surface are continually lost via redeposition on adjacent surfaces (e.g., the walls of the discharge chamber, the sample holder, and the sample surface).

* Corresponding author.
[†] NMT-1, Los Alamos National Laboratory.
[‡] LS-5, Los Alamos National Laboratory.
[§] CST-9, Los Alamos National Laboratory.
[||] University of Florida.

(1) Aston, F. W. *Isotope*, 2nd ed.; Longmans, Green and Co.: New York, 1924.
(2) Coburn, J. W.; Kay, E. *Phys. Lett.* **1971**, *19*, 350.
(3) Harrison, W. W.; Magee, C. W. *Anal. Chem.* **1974**, *46*, 1236
(4) Promotional literature: VG Elemental, Cheshire, U.K.; Finnigan-MAT, GMbH, Bremen, Germany; Kratos Analytical, Manchester, U.K., etc.
(5) Harrison, W. W. *J. Anal. Atom. Spectrom.* **1988**, *3*, 867.

10.1021/ac9810922 CCC: $18.00
Published on Web 06/16/1999

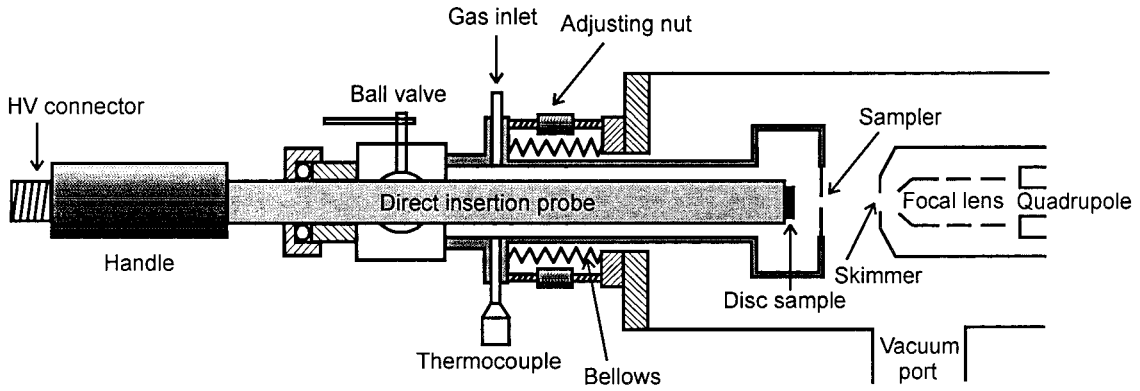

Figure 1. Schematic diagram of the source and interface region of the quadrupole GD mass spectrometer (mass analyzer stage omitted).

Table 1. Typical Operating Parameters for ICPMS and GDMS Ion Sources

param	ICPMS	GDMS
pressure (Torr)	atmospheric[6,15]	~1 [5,18]
atom density (cm^{-3})	1.5×10^{18} [15]	1×10^{16} [18]
mean free path (λ) (cm)	1.3×10^{-4}	2×10^{-2}
gas flow rate (L/min)	15 [15]	0.001 [5]
discharge power (W)	1000 [6]	3
ion density (cm^{-3})	1×10^{15} [6,15,30]	1×10^{11} [7,18]
electron density (cm^{-3})	1×10^{15} [6]	1×10^{11} [7,18]
gas temp (K)	5000 [6,15,30]	500 [5,7,36]
electron temp (eV)	1 [6,15]	0.3 [5,7]
thermal mean speed (cm/s)	1.6×10^{5}	5.2×10^{4}
collision freq (s^{-1})	1.2×10^{9}	2.6×10^{6}
plasma potential (V)	2 [6,15]	10 [5,18]

A fraction of the remaining atoms diffuse into the negative glow region of the plasma where they are ionized via interactions with numerous electrons, ions, and metastable atoms. Only the ions formed in the immediate vicinity of the exit orifice (or sampler) are likely to be extracted from the source and transmitted to the mass spectrometer.

Table 1 lists some key physical parameters of typical ICP and GD sources. Unless otherwise noted, the ICP source refers to a conventional atmospheric pressure ICP (not low-pressure, low-flow, or "cooled" ICP), and the GD source refers to dc-glow discharge optimized for use as an ionization source for mass spectrometry (not GD emission, radio frequency GD (rf-GD), or pulsed-GD). Average values are given for specific parameters to facilitate calculations presented later in this paper. Interested readers can find more information elsewhere (refs 6−8). From the data shown in Table 1, significant differences in plasma pressure and density between ICP and GD sources are readily apparent. These properties are actually advantageous for coupling the GD source with a mass spectrometer. For example, the GD source operates at relatively low pressure and requires only a single intermediate vacuum stage (second stage) between the source and the mass analyzer. The low pressure in the GD source is indirectly maintained by the vacuum in the second stage, through the sampling orifice.

In this paper, we describe the structure, performance characteristics, and theoretical considerations of the GDMS interface. Furthermore, its influence on the behavior of ions in the vicinity of the sampler orifice, sampling processes, skimming processes, mass discrimination, space charge effects, and the energy distribution of ion transport will be presented. Some theoretical background and experimental results for the ICPMS interface will be reviewed for comparison.

EXPERIMENTAL SECTION

Experiments were conducted using two GD mass spectrometers at the University of Florida. One is a prototype commercial instrument built by Finnigan-MAT (Bremen, Germany) equipped with a small quadrupole mass analyzer. The other instrument is a GD-TOFMS built in-house.[9]

Quadrupole GDMS. Figure 1 is a schematic diagram of the source and interface region of the quadrupole GD mass spectrometer. The mass analyzer is a Balzers (Hudson, NH) QMA-150 quadrupole, with an on-axis Faraday collector and a 90° off-axis electron multiplier. Parameter settings, including those for the skimmer, the ion focusing optics, the quadrupole, and the detector voltage, are provided by the program controls. The discharge parameters are manually controlled on the HV power supply, which can be operated in constant voltage, constant current, or constant power mode.

The adjustable bellows assembly (Figure 1) permits the precise alignment of the sampler orifice and the skimmer orifice to optimize ion transport into the analyzer. The sampler is a thin stainless steel plate (~0.25 mm thick) with a 0.5 mm diameter orifice. The skimmer, a flat plate with a 0.7 mm diameter central orifice, is kept at ground potential. To evaluate ion transport processes as a function of both sampler−skimmer distance and skimmer radial distance (off-axis), the position of the sampler orifice relative to the skimmer orifice was calibrated to the number of turns on the bellows screw rods.

The sample is a mixture of metal powders (Al, Cu, Ag, and W) pressed into a disk (4.5 mm o.d.; 2 mm thick) and mounted on a direct insertion probe. Two turbo pumps provide differential pumping. A needle valve is used to adjust the discharge gas (Ar) pressure to ~1 Torr in the ion source. Typical operating pressures in the second and third vacuum stage were about 1×10^{-4} and 6×10^{-6} Torr, respectively. The discharge potential was 0.8 kV, resulting in a ~4 mA sample current.

(6) Niu, H.; Houk, R. S. *Spectrochim. Acta*, **1996**, *51B*, 779.
(7) Winefordner, J. D.; Wagner, E. P., II; Smith, B. W. *J. Anal. Atom. Spectrom.* **1996**, *11*, 689.
(8) Fang, D.; Marcus, R. K. *Spectrochim. Acta* **1990**, *45B*, 1053.
(9) Hang, W.; Baker, C.; Smith, B. W.; Winefordner, J. D.; Harrison, W. W. *J. Anal. Atom. Spectrom.* **1997**, *12*, 143.

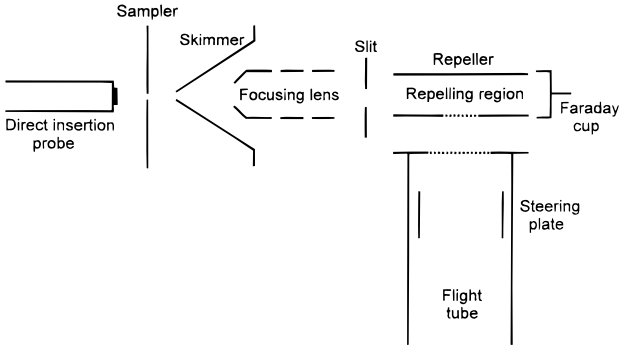

Figure 2. Schematic diagram of the GD-TOFMS (before reflector).

GD-TOFMS. The orthogonal design of the GD-TOFMS (Figure 2) permits the measurement of ion energy distributions during the experiment. The direct insertion probe and the ion source are similar to those used in the quadrupole GDMS. In the GD-TOFMS, however, the position of the sampler orifice is fixed relative to the skimmer. The sampler is a 0.5 mm thick plate with a central orifice 1 mm in diameter, and the skimmer is a 60° cone with a 1 mm diameter orifice, similar in design to the skimmer cones commonly used in ICPMS. For our experiments, typical second and third vacuum stage pressures were 1×10^{-4} and 8×10^{-6} Torr, respectively, and the discharge parameters were similar to those of the quadrupole GDMS experiments.

THEORY, RESULTS, AND DISCUSSION

Interface Design Considerations. The design of the ICPMS interface is based on the supersonic nozzle and skimmer system proposed nearly 50 years ago by Kantrowitz and Grey.[10] They found that the intensity of a molecular beam formed by a supersonic jet was several orders of magnitude greater than that of a beam emitted from an effusive source. In their design, the skimmer was located in a region of high molecular density located close to the nozzle. The angle of the skimmer cone was chosen to minimize the possibility of detached shock wave formation in front of the skimmer and to minimize reflection from its inside surface. The process of ion beam formation through supersonic expansion into a high pressure (10^{-2} to 1 Torr) environment was later investigated by Campargue.[11,12] The Campargue-type beam source then became the basis for practically all modern ICPMS instruments. Several parameters which emerged from this work (Knudson number, Debye length, gas flow rate, and shock wave structure) are critical to the generation of a particle beam for both ICPMS and GDMS interfaces, as illustrated in the following sections.

Knudson Number. The unitless Knudson number (*Kn*) describes the flow state of gas through the sampler orifice and is expressed as

$$Kn = \lambda / D_o \tag{1}$$

where λ is the mean free path and D_o is the aperture diameter. A viscous (or continuum) flow is characterized by $Kn < 0.01$, and a molecular (or effusive) flow has $Kn > 1.0$. The intermediate flow state ($0.01 < Kn < 1.0$) is termed "transition flow". Gas flow through a 1 mm ICPMS sampler orifice, at the conditions specified in Table 1, has $Kn = 1.3 \times 10^{-3}$, which falls within the viscous flow region. Using the values listed in Table 1, flow through a 0.5 mm diameter GDMS sampler has a *Kn* of 0.4 and belongs to the transition flow regime.

Debye Length. The Debye length, λ_D, is the distance over which a single ion causes a significant distortion to the applied electrostatic field[13] and is given (in centimeters) by

$$\lambda_D = 6.9(T_e / n_e)^{1/2} \tag{2}$$

where T_e is the electron temperature (K) and n_e is the electron density (particles/cm^3). For a quasi-neutral plasma, electron number density is equal to ion number density. If $\lambda_D < D_o$, the plasma will flow through the sampler orifice with no charge separation (i.e., as a bulk plasma). For both ion sources, at the conditions listed in Table 1, λ_D is considerably smaller than the orifice diameter (2.2×10^{-5} cm for ICP and 1.2×10^{-3} cm for GD). Thus, ion flow for both ICP and GD plasmas will occur with no charge separation.

Gas Flow Rates. For ICPMS, the rate of viscous gas flow through the sampler was described by Oechsner and Stumpe[14] using a supersonic nozzle interface model. This model was applied by Olivares and Houk:[15]

$$G_0 = \frac{\pi f(\gamma) N_A D_o^2 P_0}{4(MRT_0)^{1/2}} \tag{3}$$

where

$$f(\gamma) = \gamma^{1/2}\left(\frac{2}{\gamma + 1}\right)^{(\gamma+1)/[2(\gamma-1)]} \tag{4}$$

G_0 is the flow through the orifice (molecules/s), N_A is Avogadro's number, D_o is the sampler orifice diameter, P_0 is the gas pressure in the source, M is the molecular weight of the gas (40 g/mol for Ar), R is the gas constant, T_0 is the plasma temperature, and γ is the specific heat ratio (1.67 for Ar). Using the parameters listed in Table 1 for ICP, the calculated flow is 8.3×10^{20} molecules/s.

A simpler equation describing viscous gas flow through the sampler was derived by Douglas and French:[16]

$$G_0 = 0.445 n_0 a_0 D_o^2 \tag{5}$$

where

$$a_0 = [\gamma k T_0 / m]^{1/2} \tag{6}$$

and n_0 is the number density in the source (1.5×10^{18}/cm^3), a_0 is the speed of sound in the source (1.2 m/s), k is the Boltzmann

(10) Kantrowitz, A.; Grey, J. *Rev. Sci. Instrum.* **1951**, *22*, 328.
(11) Campargue, R. *J. Chem. Phys.* **1970**, *52*, 1795.
(12) Campargue, R. *J. Chem. Phys.* **1984**, *88*, 4466.
(13) Tanner, S. D.; Douglas, D. J.; French, J. B. *Appl. Spectrosc.* **1994**, *48*, 1373.
(14) Oechsner, H.; Stumpe, E. *Appl. Phys.* **1977**, *14*, 43.
(15) Olivares, J. A.; Houk, R. S. *Anal. Chem.* **1985**, *57*, 2674.
(16) Douglas, D. J.; French, J. B. *J. Anal. Atom. Spectrom.* **1988**, *3*, 743.

constant (J/k), and m is the mass of a gas molecule (6.65×10^{-26} kg for Ar). Equations 5 and 6 yield a flow rate of 8.6×10^{20} molecules/s for the ICP source, which is very similar to the result obtained using eqs 3 and 4.

In the GD source, gas flow through the sampler orifice belongs to the transition flow regime, which has not been as well-characterized as either the viscous or molecular flow conditions. For example, very little information can be found to describe the adiabatic expansion (i.e., through an orifice) from the transition state to the molecular state. If eq 5 (for viscous flow) can be applied to approximate transition flow through the GDMS sampler orifice (0.5 mm diameter), the flow rate is $\sim 5.7 \times 10^{17}$ molecules/s. For a molecular flow approximation, the rate is given by[17]

$$G_0 = C(P_0 - P_1) = 2.86(T/M)^{1/2} D_o^2 (P_0 - P_1) \qquad (7)$$

where C is the conductance of the orifice, P_1 is the pressure after the sampler, P_0 is the gas pressure inside the source, and T refers to temperature, which we assume remains constant on either side of the orifice. If $T = 400$ K,[5] the flow rate is 4.2×10^{16} molecules/s for the GDMS source at the conditions listed in Table 1.

The GD source is a closed chamber pumped through the sampler orifice, with a gas inlet controlled by a needle valve. For Ar gas at atmospheric pressure and room temperature, a 1 mL/s flow rate through the inlet is equivalent to 4.4×10^{17} molecules/s. This value is similar to the results of both of the above approximations, whether we consider the flow through the orifice to be viscous (5.7×10^{17} molecules/s) or molecular (4.2×10^{16} molecules/s). Sputtered particles in the GD source have a number density of 10^{12} /cm^3, about 4 orders of magnitude less than that of argon atoms,[18] and are consequently of minor importance.

As we can see from eq 7, the conductance (C) of a molecular flow is independent of pressure. An increase in the second stage pump speed (i.e., lower P_1) will increase neither the flow rate nor the beam velocity if P_1 is considerably smaller than P_0. Similarly, the rate equations for viscous flow (i.e., eqs 3−6) assume that $P_1 \ll P_0$; hence, P_1 is essentially zero. Thus, in both the molecular and viscous flow cases, flow rate is conductance-limited.[17]

Supersonic Expansion after the Sampler. The expansion of a free jet into a low-pressure region results in a shock wave. Inside the shock wave, the gas density decreases rapidly with increasing distance from the jet. Ashkenas and Sherman[19] derived expressions which describe the variation of Mach number, M, and the location, X_M, of the Mach disk on the axis normal to the orifice exit (Figure 3A):

$$M = 3.26\left(\frac{x_s}{D_o}\right)^{0.67} - \frac{0.61}{(x_s/D_o)^{0.67}} \qquad (8)$$

$$X_M = 0.67 D_o (P_0/P_1)^{1/2} \qquad (9)$$

where x_s is the distance from the sampler orifice. Equation 9 is valid only if $15 \le P_0/P_1 \le 1.7 \times 10^4$, which is relevant to the supersonic expansion after the GDMS sampler. For the GD source with a 0.5 mm diameter sampler orifice, eq 9 predicts that the Mach disk would be located 33.5 mm away from the sampler. Therefore, flux through the sampler would become a highly expanded (or divergent) free jet. Over the typical range of sampler−skimmer distances (6−7 mm) in the quadrupole GDMS, the Mach number will be ~10 at the skimmer orifice (eq 8).

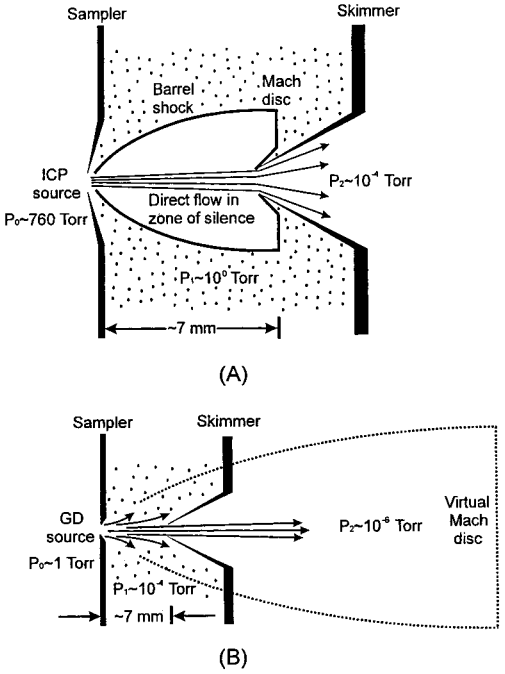

Figure 3. (A) Typical ICPMS interface; (B) typical GDMS interface.

The Campargue-type sampling process describes the supersonic expansion into a relatively high pressure (1 to 10^{-2} Torr) expansion chamber, as indicated by continuum flow regime solutions.[11,12] For a low-pressure (10^{-3} to 10^{-4} Torr) expansion chamber (e.g., the second stage in a GDMS), the supersonic jet becomes a Fenn-type expansion[20−22] (Figure 3b). For a highly expanded jet, the collision rate is sufficiently low such that continuum solutions may not be valid. The shock wave boundary layer thickness is on the order of several mean free paths under normal conditions, and the thickening of the barrel shock and Mach disk would lead to the eventual disappearance of the shock wave structure with further decreases in pressure.[19,23] At room temperature, the mean free path of argon in the GDMS expansion chamber (1×10^{-4} Torr) is 80 cm, and the shock structure is no longer detectable. Very low collision rates essentially "freeze" the expansion,[21,22] and temperature remains constant, although the density decreases as predicted by the continuum solution. About 2 mm away from the GD sampler orifice, the Mach number is approximately 4 and changes very little beyond this point.

(17) Roth, A. *Vacuum Technology*, 2nd ed.; North-Holland Publishing Co.: New York, 1982.
(18) Bogaerts, A.; Wagner, E.; Smith, B. W.; Winefordner, J. D.; Pollmann, D.; Harrison, W. W.; Gijbels, R. *Spectrochim. Acta* **1997**, *52B*, 205.
(19) Ashkenas, H.; Sherman, F. S. In *Rarefied Gas Dynamics, 4th Symposium*, Vol. II, De Leeuw, J. H., Ed.; Academic Press: New York, 1964.
(20) Fenn, J. B.; Deckers, J. In *Rarefied Gas Dynamics, 3rd Symposium*, Vol. I; Laurmann, J. A., Ed.; Academic Press: New York, 1963.
(21) Fenn, J. B.; Anderson, J. B. In *Rarefied Gas Dynamics, 4th Symposium*, Vol. II; De Leeuw, J. H., Ed.; Academic Press: New York, 1964.
(22) Anderson, J. B.; Andres, R. P.; Fenn, J. B.; Maise, G. In *Rarefied Gas Dynamics, 4th Symposium*, Vol. II; De Leeuw, J. H., Ed.; Academic Press: New York, 1964.
(23) Bier, K.; Hagena, O. F. In *Rarefied Gas Dynamics, 4th Symposium*, Vol. II; De Leeuw, J. H., Ed.; Academic Press: New York, 1964.

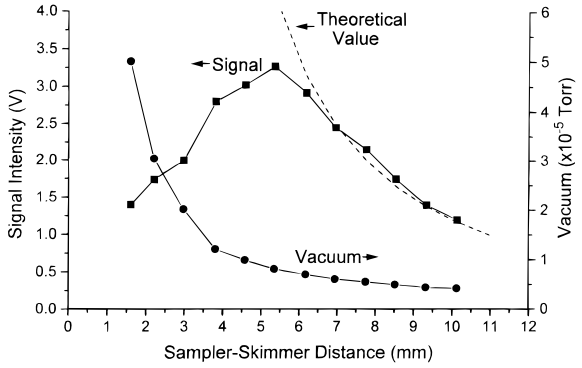

Figure 4. Plot showing the relationship between sampler−skimmer distance, signal intensity (filled squares, first *Y*-axis), and pressure in the mass analyzer (filled circles, second *Y*-axis). The sample, in this case, is a Cu disk. The dashed line represents the theoretical relationship between signal intensity and sampler−skimmer distance (eq 11).

The jet acts as a pump, which clears the background gas away from the orifice for a small distance, X_b. Downstream from this point, the density of the background gas is equal to the density outside the jet. An approximation of X_b is given as[24]

$$X_b = 0.6D_o/Kn \tag{10}$$

which, for GDMS, is about 0.75 mm. Thus, the background gas penetration is very severe in the Fenn-type shock wave structure. This is quite different from the Campargue-type expansion, where the background gas is well-isolated from both the barrel shock and the Mach disk. The gas density behind the sampler, n_s, in the Campargue-type expansion is given by[16]

$$n_s = 0.161n_0\left(\frac{X_s}{D_o}\right)^{-2} \tag{11}$$

Equation 11 also describes the axis-parallel density distribution for Fenn-type expansion and is independent of the flow state (e.g., continuum flow, transition flow, or effusive flow).[21,22,24]

The effect of the sampler−skimmer gap on signal intensity is shown in Figure 4. If the gap is too small (<6 mm), the vacuum in the last stage increases by an order of magnitude over normal operating conditions. As the vacuum in the mass analyzer degrades, transmission is reduced and signal intensity decreases. At typical sampler−skimmer distances (~7 mm), the relationship between signal intensity and sampler−skimmer spacing predicted by eq 11 is in good agreement with our experimental results (Figure 4). Experiments involving larger sampler−skimmer gaps were limited by the expansion range of the bellows assembly.

Kinetic Energy Distribution following Expansion. The continuum flow through the sampler orifice of an ICPMS has a "seeding" effect, in which heavier atoms can be accelerated to higher velocities through numerous collisions with lighter atoms. Although this effect is more pronounced when the concentration of heavy atoms is very low,[20] seeding effects are observable even when the concentration of heavy atoms (or molecules) is greater than that of the source gas.[25]

Inside the ICP source, all atoms have the same thermal kinetic energy. During the sampling process, heavy atoms are entrained along the main stream through numerous (~250, see ref 16) collisions with light atoms. Heavy atoms get most of their energy from the supersonic expansion with all atoms (or ions) ultimately moving at the speed of argon neutrals; thus, the energies of the atoms are proportional to their mass. Fulford and Douglas[26] give an approximation for the atom energy:

$$E = 0.026M \tag{12}$$

where E is energy (eV) and M is the molar mass of the atom. When considering the energy of an ion, the 2 eV plasma potential should be added.

Both the source gas density and the expansion chamber pressure in a GD source are much lower than in the ICP source. Using eqs 5 and 6[16] to estimate the number of collisions in the expansion following the GD sampler, we find that less than one collision (0.6) is experienced by each atom. If collisional energy transfer is absent, the kinetic energy of atoms passing through the sampler will be equivalent to their thermal energy while in the source. In the absence of an external electric field, the kinetic energy of the ions in the vicinity of the orifice, following the expansion, will be largely determined by the GD plasma potential, which is identical for all ions regardless of mass.

The potential applied to the steering plates of the TOFMS can serve as a measure of the relative kinetic energy for ions of different masses. For the TOFMS, the repelling region is maintained near ground. Therefore, ions receive no additional energy from the ion optics as they travel from the source to the repelling region. Each ion still has its initial kinetic energy, but with a direction perpendicular to the TOFMS axis. By applying a positive pulse to the repeller, ions are repelled and accelerated into the flight tube. The steering plate potential corresponds to the initial kinetic energy of ions, and directs ions to the detector. For ICP-TOFMS,[27] ions of different masses require different steering potentials to yield optimum signals. For GD-TOFMS, the steering potential can be optimized at the same voltage for ions of different masses (Figure 5), whether they are working gas species, sputtered species, or polyatomic species. Therefore, one can reasonably conclude that ions in the GD-TOFMS have an identical initial kinetic energy. Similar results have been obtained from a TOFMS system with an rf-GD source.[28]

Space Charge Effects. The space charge effect is severe in ICPMS.[6,29−31] In a typical ICP source (Table 1), the positive-ion current passing through the sampler is ~1.5 mA, and the Debye length ($\lambda_D \sim 10^{-3}$ to 10^{-2} mm) between the sampler and the skimmer is much smaller than the diameter of the skimmer

(24) Anderson, J. B. Molecular Beams From a Nozzle Source. In *Molecular Beams and Low-Density Gas Dynamics*; Wegener, P. P., Ed.; Marcel Dekker: New York, 1974.
(25) Becker, E. W.; Henkes, W. *Z. Phys.* **1956**, *146*, 320.
(26) Fulford, J. E.; Douglas, D. J. *Appl. Spectrosc.* **1986**, *40*, 971.
(27) Myers, D. P.; Li, G.; Yang, P.; Hieftje, G. M. *J. Am. Soc. Mass Spectrom.* **1994**, *5*, 1008.
(28) Myers, D. P.; Heintz, M. J.; Mahoney, P. P.; Li, G.; Hieftje, G. M. *Appl. Spectrosc.* **1994**, *48*, 1337.
(29) Chen, X.; Houk, R. S. *Spectrochim. Acta* **1996**, *51B*, 41.
(30) Li, G.; Duan, Y.; Hieftje, G. M. *J. Mass Spectrom.* **1995**, *30*, 841.
(31) Gillson, G. R.; Douglas, D. J.; Fulford, J. E.; Halligan, K. W.; Tanner, S. D. *Anal. Chem.* **1988**, *60*, 1472.

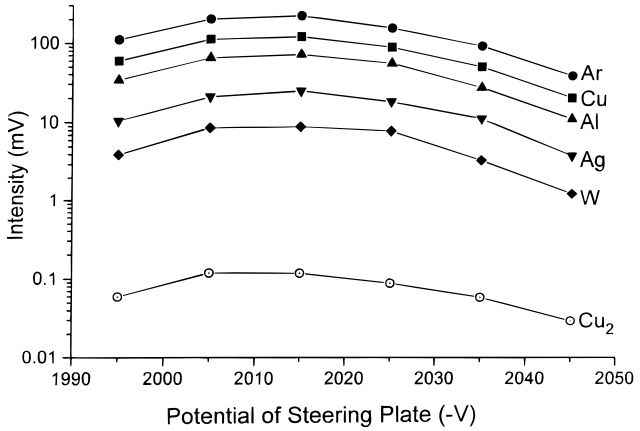

Figure 5. Plot showing the relationship between steering plate potential (negative) and signal intensities (Ar, Al, Cu, Ag, W, and Cu_2). The sample is a mixed metal powder disk.

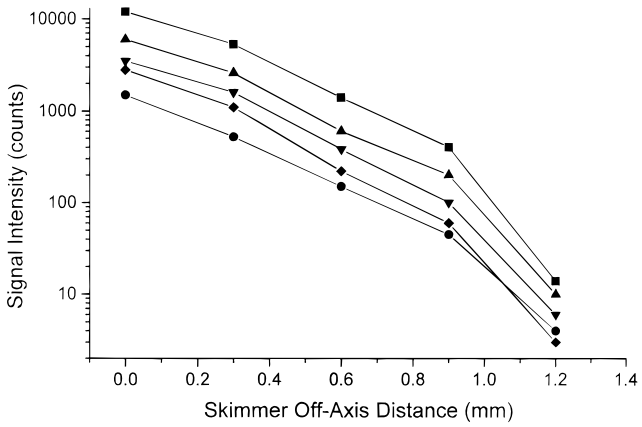

Figure 6. Plot of signal intensities for ^{36}Ar, Al, Cu, Ag, and W as a function of radial offset between the sampler and the skimmer. The sample is a mixed metal powder disk.

orifice. Thus, the sampled plasma remains a quasi-plasma. After the plasma is ejected through the skimmer, ion density decreases and λ_D increases, resulting in space charge separation. Consequently, low-mass ions are repelled from the axis, causing a mass bias.

The significance of the space charge can be evaluated by the perveance, P,[29,32] which is defined as

$$P = I/V^{3/2} \tag{13}$$

where I is the ion current in amperes and V is the acceleration potential in volts. If a beam of singly charged positive ions is to have a negligible space charge effect, the following relation must be satisfied:

$$P_{max} = 10^{-8}\left(\frac{m_{ion}}{m_e}\right)^{-1/2} \tag{14}$$

where m_{ion} is the ion mass and m_e is the electron mass. Thus, for argon ions, P_{max} is 3.7×10^{-11}. If the flow rate through the GDMS sampler is 4.4×10^{18} molecules/s, and if we assume an ion-to-atom ratio of 1×10^{-5}, the resulting positive-ion current is ~5 μA. For a plasma potential of 10 V, P is 1.6×10^{-7}, which exceeds P_{max} by 3 orders of magnitude. The plasma flowing through the sampler is a bulk plasma with λ_D of 1.2×10^{-2} mm at the sampler orifice. However, the electron density in the region between the sampler and the skimmer (the expansion chamber) is unknown, and no experimental data for this parameter exist. Therefore the value of λ_D after the sampler is unknown.

Figure 6 shows the variation in signal intensity as a function of the radial (off-axis) offset of the skimmer away from the sampler orifice. The sampler−skimmer distance is fixed at 6.5 mm. Trends in ion signal intensity with increasing offset distance for light (Ar, Al) and heavy (Ag, W) ions are very similar. Thus, mass bias does not occur within the ion beam, normal to its axis. If charge separation had occurred and caused the space charge effect, the ratio of light ions to heavy ions would increase as the radial offset distance increased. These results suggest that the space charge effect does not occur in the quadrupole GDMS expansion chamber as long as the sampler−skimmer distance is 6−7 mm. Downstream from the skimmer, λ_D exceeds the orifice diameter, and charge separation should occur.

The exact distance where charge separation would occur in the quadrupole GDMS is unknown. Estimates based on the positive ion current collected on the Faraday cup in the GD-TOFMS indicate that the ion current passing though the skimmer orifice is ~20 nA. The perveance, P, for a 20 nA current is 6.3×10^{-10}, about 17 times greater than P_{max} for Ar ions. Therefore, in the GD-TOFMS, the space charge effect occurs during the skimming process, causing beam spreading and decreased transmission. However, space charge effects in GDMS may not be as severe as for the ICPMS due to the lower total ion current (see below).

If we assume that ions pass through a skimmer orifice of diameter D_m and then drift through a field-free distance, L, the resulting beam is spread out by Coulombic repulsion to diameter D_L. The total beam divergence can be estimated by[30,33]

$$\frac{D_L}{D_m} = \left[3.3 \times 10^{12}\left(\frac{L}{D_m}\right)^2\left(\frac{1}{v}\right)^3\left(\frac{z}{M}\right)I\right] + 1 \tag{15}$$

where I is the ion beam current (μA), v is the ion velocity (m/s), and z is the charge on the ion (singly charged for GD source, $z = +1$). The initial kinetic energy of all ions in the GDMS is determined by the plasma potential V_P (=10 V), and v can be expressed as

$$v = [2eV_p/m]^{1/2} = 4.4 \times 10^4 M^{-1/2} \tag{16}$$

where e is the charge on a single electron (1.6×10^{-19} C). Then, eq 15 can be rewritten as

$$\frac{D_L}{D_m} = \left[3.9 \times 10^{-2}\left(\frac{L}{D_m}\right)^2 M^{1/2} I\right] + 1 \tag{17}$$

Thus, beam divergence in GDMS is proportional to the square root of the ion mass. This is not the case for ICPMS, where beam

(32) Szilagyi, M. *Electron and Ion Optics*; Plenum Press: New York, 1988.

divergence is *inversely* proportional to the ion mass.[29,30] The magnitude of postskimmer beam divergence is also much smaller for GDMS than for ICPMS. If a GDMS has a total ion current (postskimmer) of ~20 nA and if $L = 10$ mm and $D_m = 1$ mm, then D_L is 1.41, 1.48, and 3.43 for Li^+, Ar^+, and U^+, respectively. For an ICP source with an ion current of ~6 μA (postskimmer), the magnitude of D_L is 10^2 to 10^3 times greater for the same elements.[31] In practice, beam divergence in ICP and GD is reduced by using extraction lenses after the skimmer.[30]

Equation 17 also indicates that, for GDMS, space charge effects repel heavy ions farther from the beam axis than light ions. This phenomenon would become more pronounced at larger ion currents and may be apparent in trends observed for relative sensitivity factors (RSFs) acquired using GDMS.[34] The definition of RSF in ref 33 is the reciprocal of that used by Vieth and Huneke,[35] such that larger RSFs reflect higher sensitivity. These results indicated that RSFs for most heavy ions were consistently <1 in a 4 mm dc discharge. Smaller RSFs were obtained when data were acquired in microsecond pulsed mode with a pulse current of 30 mA.

Skimmer Design and Ion Extraction. Another limitation of the ICP source is the difficulty with which an intense ion beam is passed through the skimmer. Both atoms and ions scatter off-axis due to wave-front-like disturbances caused by the reflection of atoms in front of the skimmer. The oblique wave front along the conical internal wall may extend into the beam axis and degrade transmission, even if the skimmer has an optimized angle (50−60°)[12] and a very sharp tip.

In GDMS, flow through the skimmer orifice is free molecular flow. Atoms which collide with the external surface are reflected back into the flow, but their density is sufficiently low such that collisions with approaching atoms (or ions) are negligible. The neutral beam divergence following the skimmer, in molecular flow, is smaller than for either continuum flow or transition flow (Figure 3). Campargue[12] has shown that variation in the skimmer angle effects beam divergence only slightly at an expansion chamber pressure of 2.9×10^{-3} Torr and that such effects are not observable at 7×10^{-4} Torr. Thus, empirically derived flat skimmer designs are correct in theory.[3] A novel flat skimmer design using a 15 cm sampler−skimmer distance, and an intermediate Einzel lens for beam focusing, also works quite successfully.[36]

An additional advantage of the GDMS skimmer is that a negative voltage can be applied to repel electrons and attract ions through the skimmer orifice. This functions more effectively for a conical skimmer[37] and also reduces mass bias caused by the space charge effect. When −1.0 kV is applied to the skimmer, we observed nearly constant signal intensity as the sampler−skimmer distance was increased from 5 to 8 mm. The mean free path lengths in the TOFMS are 5.3 and 10 m, respectively, due to the pressure change. A bias applied to the skimmer in ICPMS may result in the production of a glow discharge, which complicates the spectrum and increases the background noise.[15] However, some recent successes using this approach for ICPMS have been documented.[38]

CONCLUSIONS

In this paper, a survey of theoretical considerations combined with preliminary experimental results, we have addressed several problems. Our findings indicate that there are distinct and fundamental differences between glow discharge and inductively coupled plasma ion sources, which are relevant to both ion sampling and ion extraction processes. In a typical GDMS ion source, transition flow is transformed to molecular flow as the plasma passes through the sampler orifice. Shock wave fronts do not occur in the supersonic expansion of the GD ion source, which permits greater flexibility for skimmer design. However, if the sampler−skimmer spacing is <6 mm, analyzer pressure rises, and ion transmission is severely reduced. Finally, we have shown that ions of different masses have similar initial kinetic energies in the GD ion source. Therefore, the angle of the skimmer cone is not a critical parameter for optimal ion beam extraction.

These results have a direct impact on analytical instrumentation design. In GD ion sources, ions of different masses have similar energies (a requirement of orthogonal TOFMS systems); thus, it is not necessary to couple a GD source with an on-axis TOFMS. The space charge effect would still be problematic, even though the ion current emanating from a GD source is several orders of magnitude lower than that of ICPMS. However, theoretical calculations (eq 17) suggest that space charge effects in GDMS repel *heavy* ions farther off-axis than light ions. Reduction of the space charge effect would reduce the total range of RSF values for a given sample and could be achieved by limiting the ion current through the sampler. Ion current could be decreased either by decreasing the GD potential or by reducing the sampler orifice size but would sacrifice a degree of analytical sensitivity. Further studies of ion and electron densities beyond the sampler and the skimmer would provide a more convincing explanation of the space charge effects in GD ion sources, as predicted by eq 17.

Another common problem encountered in analytical GDMS is isobaric interference due to polyatomic clusters (e.g., $[MAr]^+$, $[MM]^+$), which increases detection limits and decreases analytical sensitivity for some elements. Polyatomic species may be formed in the GD source, but clusters may also form as a result of condensation caused by the "freezing" phenomenon in the expansion chamber (between the sampler and the skimmer). If the condensation effect is highly efficient, the rate of production of clusters may be significant even though the actual number of collisions in the expansion chamber is very low. Although the data presented here are insufficient to prove this possibility, condensation effects may produce a significant number of polyatoms during expansion, and an additional pumping stage could be used to introduce the beam more gradually into the mass analyzer and reduce the number of polyatomic species.

Received for review October 1, 1998. Accepted April 16, 1999.

AC9810922

(33) Weber, C. *Focusing of Charged Particles*, Vol. I; Academic Press: New York, 1967.

(34) Hang, W.; Harrison, W. W. *98 Winter Conference on Plasma Spectroscopy*, S2, Scottsdale, AZ, 1998. Hang, W.; Yan, X.; Ingeneri, K.; Harrison, W. W. Unpublished data.

(35) Vieth, W.; Huneke, J. C. *Spectrochim. Acta* **1991**, *46B*, 137.

(36) Hang, W.; Harrison, W. W. *Anal. Chem.* **1997**, *69*, 4957.

(37) Turner, P. J. Some Observations on Mass Bias Effects Occurring in ICPMS Systems. In *Applications of Plasma Source Mass Spectrometry*; Holland, G., Eaton, A. N., Eds.; Royal Society of Chemistry: Cambridge, U.K., 1991.

(38) Hu, K.; Houk, R. S. *J. Am. Soc. Mass Spectrom.* **1993**, *4*, 733.